Mutations of the central tyrosines of putative Cholesterol Recognition Amino acid Consensus (CRAC) sequences modify folding, activity, and sterol-sensing of the human ABCG2 multidrug transporter

Zita Gál[a], Csilla Hegedüs[a,b], Gergely Szakács[a], András Váradi[a], Balázs Sarkadi[a,b] and Csilla Özvegy-Laczka[a,*]

[a]Institute of Enzymology, Research Centre for Natural Sciences, Hungarian Academy of Sciences, Magyar tudósok körútja 2., H-1117 Budapest, Hungary
[b]Molecular Biophysics Research Group, Hungarian Academy of Sciences and Semmelweis University, Diószegi út 64., H-1113 Budapest, Hungary

Short title: CRAC motifs in ABCG2

[*]**Corresponding author:** Csilla Özvegy-Laczka, Institute of Enzymology, Research Centre for Natural Sciences, Hungarian Academy of Sciences, Magyar tudósok körútja 2., H-1117 Budapest, Hungary, Phone: +36 1 3826715, FAX: +361 3826295
e-mail: laczka.csilla@ttk.mta.hu

Abbreviations: CA, cholic acid; CRAC, cholesterol recognition amino acid consensus; DOX, doxorubicin; FBS, fetal bovine serum; FLP, flavopiridol; GC, glycocholate; HRP, horseradish peroxidase; MTX, methotrexate, PBS, Phosphate Buffered Saline, RAMEB, Randomly Methylated β-Cyclodextrin; SN-38, 7-Ethyl-10-hydroxycamptothecin; TC, taurocholate; TOP, topotecan.

ABSTRACT

Human ABCG2 is a plasma membrane glycoprotein causing multidrug resistance in cancer. Membrane cholesterol and bile acids are efficient regulators of ABCG2 function while the molecular nature of the sterol-sensing sites has not been elucidated. The Cholesterol Recognition Amino acid Consensus (CRAC, L/V-$(X)_{(1-5)}$-Y-$(X)_{(1-5)}$-R/K) sequence is one of the conserved motifs involved in cholesterol binding in several proteins. We have identified five potential CRAC motifs in the transmembrane domain of the human ABCG2 protein. In order to define their roles in sterol sensing, the central tyrosines of these CRACs (Y413, 459, 469, 570 and 645) were mutated to S or F, and the mutants were expressed both in insect and mammalian cells. We found that mutation in Y459 prevented protein expression; the Y469S and Y645S mutants lost their activity; while the Y570S, Y469F, and Y645F mutants retained function as well as cholesterol and bile acid sensitivity. We found that in the case of the Y413S mutant, drug transport was efficient, while modulation of the ATPase activity by cholesterol and bile acids was significantly altered. We suggest that the Y413 residue within a putative CRAC motif has a role in sterol-sensing and the ATPase / drug transport coupling in the ABCG2 multidrug transporter.

Keywords: ABCG2, multidrug resistance, cholesterol, bile acids, cholesterol recognition amino acid consensus

1. **Introduction**

ABCG2 is a plasma membrane glycoprotein in the ABC (ATP Binding Cassette) family of proteins that are characterized by a unique nucleotide binding/hydrolyzing domain (NBD) and hydrophobic membrane spanning sequences (transmembrane domain, TMD), mediating ATPase activity and the recognition and translocation of transported substrates, respectively. Several ABC transporters, called multidrug resistance (MDR) proteins, extrude various chemically unrelated compounds from the cells by utilizing the energy of ATP hydrolysis. ABCG2 is an MDR half transporter, harboring only a single NBD and a single TMD, and must at least homodimerize to exert its proper transporter function [1-3].

ABCG2 is expressed in many tissues, most abundantly in organs displaying barrier functions (brain, placenta, and intestine) where it influences the passage of hydrophobic or slightly negatively charged molecules, including numerous drugs and food constituents. Therefore, ABCG2 can significantly influence the ADME-Tox (Absorption, Distribution, Metabolism, Excretion and Toxicity) properties of drugs, especially the absorption from the intestine, penetration to the central nervous system through the blood-brain-barrier, or the elimination from the liver or kidney [3-6]. Optimal activity of ABCG2 has been shown to be important in the regulation of serum urate levels, and polymorphic ABCG2 variants with decreased function or expression were shown to be associated with a higher risk of gout [7-9]. Human ABCG2 is expressed in stem cells of various origins, where it provides a protective role under hypoxic conditions [10]. Overexpression of ABCG2 confers multidrug resistance to cancer cells [11-13].

We and others have shown that both the ATPase and the transport activity of ABCG2 are significantly accelerated by cholesterol enrichment of "cholesterol poor" insect cell membranes; whereas cholesterol depletion of mammalian cells results in decreased ABCG2 function [14, 15], implying that cholesterol is a major modulator of ABCG2 function. Subsequent studies have shown that functional reconstitution of purified ABCG2 requires cholesterol, suggesting that it is in fact essential for ABCG2 activity [16].

The mechanisms by which cholesterol-ABCG2 interactions translate into the observed changes of function, or the site(s) involved in cholesterol sensing have not been defined. There is no experimental evidence proving direct binding of cholesterol by ABCG2 and it is not known if ABCG2 recognizes cholesterol as a transported substrate, as shown for some related ABCG transporters [17, 18]. More probably, cholesterol is an allosteric modulator of the

transporter, or may also have an indirect effect through influencing the biophysical properties of the lipid bilayer.

Previous studies have suggested that single amino acids can influence cholesterol sensing of ABCG2. Mutation of R482 to small amino acids (D, G, N, S, T) were shown to alter the cholesterol sensitivity [19]; mutation of the leucines in the LxxL motif (potential steroid binding element (aa 555-558 [20]) resulted in an apparent cholesterol insensitivity of ABCG2 in Sf9 membranes [19]. While these results may suggest that the mutated amino acids directly participate in cholesterol binding, they are not part of known motifs that characterize dedicated cholesterol binding regions. Many proteins that interact with cholesterol possess an amino acid consensus sequence termed "CRAC" (Cholesterol Recognition Amino acid Consensus) with the pattern (L/V-$(X)_{(1-5)}$-Y-$(X)_{(1-5)}$-R/K). The CRAC sequence was shown to be an essential determinant of cholesterol recognition in the peripheral-type benzodiazepine receptor, caveolin, the gp41protein of the HIV virus, or an integral outer mitochondrial membrane translocator protein [21-24]. The length of a CRAC motif varies between 5-13 amino acids, however, only the first and last amino acids and the central tyrosine residue are conserved. Various mutational studies of the CRAC motifs of cholesterol binding proteins and cholesterol-regulated ion channels have demonstrated the crucial role of the central tyrosine in cholesterol binding [22, 23, 25].

Given the modulatory effects of cholesterol on ABCG2 activity, we screened the amino acid sequence of the protein for CRAC motifs. We have identified five putative CRAC sequences, and changed the central tyrosines to define each motif's role in cholesterol-sensing. Here we show that the CRAC motif containing tyrosine at position 413 in transmembrane helix 1, is involved in sterol sensing and the modulation of ATPase / transport coupling of the ABCG2 transporter.

2. **Experimental procedures**

2.1. Materials - Cholesterol-RAMEB (Randomly Methylated β-Cyclodextrin) was a kind gift from Cyclolab Hungary. All other chemicals were purchased from Sigma (Sigma Aldrich, Hungary) unless stated otherwise.

2.2. Plasmid constructs - For the expression of ABCG2 mutants in insect cells, baculovirus plasmids containing the appropriate mutant ABCG2 cDNAs were generated by PCR mutagenesis, as described earlier [26]. The list of primers used for mutagenesis is provided in the "Supplementary material". The PCR products were digested with PstI and NcoI enzymes and were ligated into the corresponding sites of the pAcUW21-L/wtABCG2 plasmid [27]. The base order of the constructs was confirmed by sequencing. The generation of the vector construct with the ABCG2-K86M mutant was described earlier [26].

The plasmids for stable expression in mammalian cell lines were created by the ligation of the appropriate fragments from pAcUW21-L/ABCG2-Tyr mutant between the NotI-BamHI sites of the pSB-CMV-wtABCG2 plasmid [28].

2.3. Cells and cell lines - Sf9 cells (Invitrogen, Life technologies) were grown in TNM-FH insect cell medium complemented with 10 % FBS and 100 μg/ml penicillin/100 U/ml streptomycin at 27ºC. HEK 293 cells were cultured in D-MEM medium containing 10 % FBS and 100 μg/ml penicillin/100 U/ml streptomycin and 5 mM glutamin at 37ºC in 5% CO_2.

2.4. Generation of insect cells expressing ABCG2-Tyr mutants - Sf9 cells were co-transfected with 250 ng linearized baculovirus DNA + 250 ng baculovirus plasmid DNA using the BaculoGold transfection kit following the protocol provided by the supplier (BD Biosciences). The presence of the engineered mutations was verified by restriction endonuclease digestion of the PCR-amplified ABCG2 DNA.

2.5. Generation of HEK 293 cells stably overexpressing human ABCG2 and its Tyr mutants - Cells were transfected using 3 μl Fugene6 reagent (Promega) and 500 ng of the Sleeping Beauty pSB-ABCG2 plasmid DNA and 500 ng plasmid coding a transposase [29]. 48h post transfection the cells were cultured in 1 μg/ml puromycin for 14 days. Cells overexpressing the highest amounts of the appropriate ABCG2 variant were sorted based on 5D3 labeling using FACSAria cell sorter (Becton Dickinson). In cholesterol depletion experiments we used the HEK 293 cell line stably expressing the R482G mutant established earlier [15].

2.6. Membrane preparation – Isolation of membranes from Sf9 cells expressing human ABCG2 or its Tyr mutants and the determination of membrane protein concentrations by the modified Lowry method were performed as described [30]. Besides control membranes prepared from untreated Sf9 cells, cholesterol pre-loaded membranes were also generated by co-incubation of the membranes with 0.25, 0.5, 1 or 2 mM cholesterol-RAMEB at 0°C for 30 minutes prior to the final ultracentrifugation step of the membrane preparation procedure [15].

2.7. Detection of ABCG2 by Western blotting - Sf9 membranes or HEK 293 whole cells were suspended in sample loading buffer (62.5 μM Tris HCl pH 6.8, 2 % SDS, 10 μM EDTA-Na pH 6.8, 10 % glycerol, 2M urea, 0.14 mg/ml bromophenol blue, 100 μM dithiothreitol). Protein samples were separated on 7.5% Laemmli gels. Western blot analysis was performed as described earlier [26], by using the BXP-21 monoclonal antibody in a 2,000x dilution, and a goat anti-mouse HRP-conjugated secondary antibody (10,000x dilution, Jackson Immunoresearch).

2.8. BXP-21 or 5D3 labeling - 5 x 10^5 HEK 293 cells were incubated in 1 ml HPMI buffer (120 mM NaCl, 5 mM KCl, 400 μM $MgCl_2$, 40 μM $CaCl_2$, 10 mM Hepes, 10 mM $NaHCO_3$, 10 mM glucose and 5 mM Na_2HPO_4 pH7.4), containing 0.5% bovine serum albumin and 1 μg/ml 5D3 antibody for 30 min at 37°C in the presence of 1 μM Ko143. After washing, the cells were further incubated with a secondary, phycoerythrin-conjugated anti-mouse antibody (Molecular Probes, 2 μg/ml). Fluorescence was analyzed in an Attune focusing flow cytometer (Applied Biosystems).

When Sf9 membranes were labeled with anti-ABCG2 antibodies, 90 μg membranes were incubated with BXP-21 (100x dilution) or 5D3 (final concentration 2 μg/ml) antibody in a buffer containing 40 mM MOPS-Tris, 50 mM KCl and 500 μM EGTA-Tris for 30 minutes at 37°C, and after washing with phycoerythrin-conjugated goat anti-mouse antibody (final concentration 1 μg/ml) for additional 30 minutes at 37°C. Fluorescence was analyzed in a FACSCalibur cytometer (BD Biosciences) [15, 31].

2.9. ATPase assay - Measurement of ATP hydrolysis was performed as described earlier [27]. The concentrations of test compounds used in the different experiments are indicated in the figure legends. Basal or drug-stimulated ATPase activities were compared to that measured in the absence of excess cholesterol. For the calculation of the K_A values, the data were fitted with a non-linear dose response curve using the Origin 8.6 program.

2.10. Vesicular uptake assay - The accumulation of 50 μM ^{3}H-methotrexate was measured for 10 minutes at 37°C, and the transport reaction was terminated by rapid filtration [32]. ATP-

dependent transport was determined by subtracting the transport measured in the absence of MgATP from that of measured in the presence of 4 mM MgATP.

2.11. Cellular uptake of Hoechst 33342, BODIPY-prazosin, Pheophorbide A and mitoxantrone – Accumulation of 1 μM Hoechst 33342, 20 nM BODIPY-prazosin, 2 μM Pheophorbide A or 5 μM mitoxantrone was measured as described earlier [26]. Briefly, 5 x 10^5 HEK 293 cells were co-incubated with the given compound at 37ºC for 20 (Hoechst 33342 and BODIPY-prazosin) or 30 (Pheophorbide A and mitoxantrone) minutes. The reaction was terminated by the addition of ice-cold PBS. After centrifugation at 100 g for 5 minutes at 4ºC, the cells were suspended in 1 ml PBS containing 1.25 μg/ml propidium iodide and intracellular fluorescence was measured in an Attune (Hoechst 33342 and BODIPY-prazosin) or FACSCalibur (Pheophorbide A and mitoxantrone) cytometer. In the case of Hoechst 33342, cellular fluorescence "transport factor" was calculated as follows: $(F_{100}-F_0)/F_{100}*100$, where F_0 is the fluorescence (mean values) of Hoechst 33342 in the absence of an inhibitor; F_{100} is the fluorescence (mean values) in the presence of 1 μM Ko143.

2.12. Cholesterol depletion - 1 x 10^6 HEK 293 cells were incubated with 0.9 ml 4 mM empty RAMEB diluted in HPMI for 30 minutes at 37ºC. Then RAMEB was removed by centrifugation at 700 g for 5 minutes at room temperature, and the transport experiment was performed as described above.

2.13. Determination of doxorubicin efflux - 5 x 10^5 HEK 293 cells were incubated with 5 μM doxorubicin in a final volume of 100 μl for 30 minutes at 37ºC in the presence or absence of 1 μM Ko143. After washing the cells with 1 ml HPMI, the cells were further incubated in 100 μl HPMI with or without 1 μM Ko143 for 30 minutes at 37ºC. The reaction was stopped by washing the cells with 1 ml ice-cold PBS. After centrifugation at 100 g for 5 minutes at 4ºC, the cells were suspended in 1 ml PBS containing 1.25 μg/ml propidium iodide and intracellular fluorescence was measured in an Attune flow cytometer at Ex/Em= 488 nm/574 nm.

2.14. Cytotoxicity assay – 3 x 10^3 HEK 293 cells were seeded on flat bottom 96-well plates one day prior to the addition of the given drug. On day 0 drugs were pipetted onto the cells; at 72h the supernatant was removed and 100 μl 5% PrestoBlue (Life Technologies) was added to the cells. After incubation at 37ºC, 5% CO_2 for 1.5 hours, metabolized PrestoBlue was measured in a Perkin Elmer Victor X3 2030 Multilabel Plate Reader at 540 nm excitation and 579 nm emission wavelengths.

2.15. Statistical analysis of data – Statistical significance was assessed using paired Student's t-test.

3. Results

3.1. Identification of potential CRAC motifs

Cholesterol sensor motifs are located in or near the membrane plane; therefore we restricted our analysis to the transmembrane domain of ABCG2. We identified five putative CRAC motifs in ABCG2 (Fig. 1). Alignment of the corresponding regions of the human ABCG proteins revealed that three out of the five identified CRAC motifs are also present in other members of the human ABCG family (see Figure 1, insert). The putative CRAC motifs identified in the sequence of human ABCG2 are also present in ABCG2 homologs. The 1st CRAC motif (aa 407-418) is conserved amongst mammals (with the exception of rhesus monkey), but is absent in chicken, or lower species. The 2nd and 3rd potential CRAC motifs (aa 454-465 and 466-473, respectively) can be found even in various fish, e.g. Atlantic salmon or Rainbow trout; the 4th and 5th putative CRAC motifs (aa 564-575 and 641-647, respectively) are conserved amongst vertebrates.

3.2. Expression and ATPase activity of ABCG2 CRAC mutants in Sf9 insect cells

To analyze whether the putative CRAC motifs of ABCG2 influence cholesterol-sensing, we mutated the central tyrosines (Y413, 459, 469, 570 and 645) to Ser. The mutant proteins were expressed in Sf9 insect cells for functional measurements. All but one of the ABCG2 mutants were successfully expressed in Sf9 insect cells. Mutation of Y459 to S prevented the expression of the protein, precluding this mutant from further analysis (Fig. 2A).

Transport of substrates by ABCG2 is coupled to the hydrolysis of ATP. Measurement of the ATPase activity of the transporter is a well-established tool for the characterization of the activity of various mutant protein variants as well as for the screening of potential ABCG2-interacting compounds [5]. In order to determine the functionality and the cholesterol dependence of the CRAC mutant ABCG2 proteins, we measured their ATP hydrolytic capacity in isolated Sf9 insect cell membranes. We found that mutation of Tyr to Ser at position 469 or 645 resulted in the loss of ATP hydrolysis (even if the activity is corrected for the lower expression level of the Y469S mutant); while mutations in the other two positions apparently did not alter ABCG2 functionality, as both the Y413S and Y570S mutants showed a high level of ATPase activity, inhibited by a general ATPase inhibitor vanadate or the specific ABCG2 inhibitor Ko143 (Fig. 2B).

In order to test if the inactivity of the Y469S and Y645S mutants was due to a specific loss of Tyr at this position, we also mutated these tyrosines to phenylalanines. We found that the Y469F and Y645F mutants were active (Fig. 2B), indicating the importance of the phenyl ring, but not of a hydroxyl group at these positions.

3.3. Effects of cholesterol on the ATPase activity of the CRAC mutants

To test whether the CRAC tyrosine mutants are sensitive to the cholesterol content of the membranes, we characterized their ATPase activity in cholesterol-enriched insect cell membranes (Fig. 2C). The cholesterol content of the insect cell membranes is relatively low, as compared to mammalian cells (5-8 μg cholesterol/mg membrane protein vs. 50 μg cholesterol/mg membrane protein in insect and mammalian cells, respectively). Co-incubation with cholesterol-loaded cyclodextrin complexes was shown to be a reliable experimental tool to increase the cholesterol contents of Sf9 membranes by up to 10-fold [15]. Using this approach, we have shown that the ATPase activity, especially the activation of ATP hydrolysis by transported substrates, in the case of the wild-type ABCG2 is greatly enhanced when the Sf9 membranes are enriched in cholesterol (see [15] and Fig. 2C and Fig. 3A).

We found that the basal ATPase activity of the Y469F, Y570S and Y645F mutants showed a moderate (approximately 20%, $p<0.05$) increase upon cholesterol addition, while the substrate stimulated ATP hydrolysis of the same mutants was significantly (50-100% increase, $p<0.01$) accelerated by cholesterol loading (Fig. 2C). Therefore, these CRAC mutants behaved similarly to the wild-type ABCG2 protein. These results argue against a role of tyrosines 469, 570 and 645 in cholesterol sensing, suggesting that the corresponding regions are not functional CRAC motifs.

Conversely, we found that in the presence of cholesterol, the ATPase activity of ABCG2-Y413S was distinct from that of the wild-type transporter. In the case of Y413S, cholesterol resulted in a major (50 +/- 8 %; $p<0.01$) enhancement of the basal ATP hydrolysis, which could be only slightly stimulated by the addition of prazosin or quercetin (Fig. 2B and C, and Fig. 4B).

Next, we investigated whether other compounds which are known substrates of wtABCG2 also differently modify the Y413S-ATPase in the presence of cholesterol (Fig. 3). Again, cholesterol potentiated the drug-stimulated ATPase activity of the wild-type (Fig. 3A), as well as the 469F, the 570S and 645F mutants in the presence of several substrates (Supplementary Figure S1). In contrast, the Y413S mutant had a significantly altered ATPase modulation pattern. Quercetin showed a 30 +/- 6.5 % stimulation ($p<0.01$), whereas doxorubicin,

flavopiridol, topotecan and SN-38 resulted in a concentration dependent inhibition (ranging from 26-70 %) of the ATPase activity of the protein (Fig. 3B, C, D and not shown).

For a detailed analysis of the effects of cholesterol loading, the basal and drug-stimulated ATPase activities of the wild-type and Y413S ABCG2 mutants were compared at increasing membrane cholesterol concentrations. As shown in Fig. 4A, the baseline ATPase of Y413S is activated by lower cholesterol concentrations than that of the wild-type protein, with a lower apparent half-maximum cholesterol activation concentration (K_A value of 0.37 +/- 0.27 mM) as compared to the apparent affinity of the wild-type protein (K_A for cholesterol of 0.70 +/- 0.09 mM). In contrast, in the case of the substrate-stimulated ATPase activities, wtABCG2 showed higher sensitivity to cholesterol loading (Fig. 4B): in the presence of quercetin the calculated K_A value for cholesterol activation of the wild-type protein was 0.22 +/- 0.20 mM, while, due to the low level of cholesterol activation a reliable K_A for the Y413S protein could not be determined.

3.4. Altered bile acid sensitivity of the ABCG2-Y413S mutant

The experiments described above showed that both the baseline ATPase activity and also the stimulation of the baseline ATP hydrolysis by various drugs of the Y413S mutant differ significantly from that of the wild-type protein when excess cholesterol is present. We have recently found that bile acids (steroids formed from cholesterol in the liver) significantly decrease the high basal ATPase activity of wtABCG2, while they do not interfere with the ABCG2-mediated ATP hydrolysis measured in the presence of substrates [16, 19]. This phenomenon results in a significant (up to 5-7 fold) increase in the relative, substrate stimulated ATP hydrolysis, depending on the type of bile acids. In order to find out whether the active ABCG2 CRAC mutants have any alterations in their interactions with bile acids, we measured their ATPase activities in the presence of cholic acid, glycocholate and taurocholate.

We found that the ATPase activities of the 570S, 469F, 645F and wild-type ABCG2 variants were similarly modified by bile acids (data not shown). In contrast, we found major differences in the effects of bile acids on the ATPase activity of the Y413S mutant. Though the addition of bile acids decreased the baseline ATPase activity of this ABCG2 mutant (Fig. 5A), bile acids also decreased ATP hydrolysis in the presence of substrates. Therefore the net result of bile acid effects was only a slight increase in the relative substrate stimulation of the Y413S mutant (Fig. 5B-D).

3.5. Effects of cholesterol on the transport activity of the ABCG2 CRAC mutants in Sf9 membranes

In addition to its effect on the ABCG2-ATPase activity, cholesterol has also been shown to significantly enhance the transport capacity of the protein – e.g. methotrexate transport by the wild-type ABCG2 was about 4-fold activated when the insect cell membrane vesicles were enriched in cholesterol [15]. To further analyze the consequence of the putative CRAC Tyr mutations on the cholesterol-sensing of ABCG2, we measured ^{3}H-methotrexate transport both in control and cholesterol-loaded Sf9 membrane vesicles. As documented in Fig. 6, all the examined ABCG2 mutants, including Y413S, exhibited a methotrexate transport activity that, similarly to the wild-type transporter, was significantly (3-4 fold) enhanced by cholesterol loading of the membranes.

3.6. Expression and transport activity of ABCG2 CRAC mutants in HEK 293 cells – effect of cholesterol depletion

According to the presented results the baseline ATPase activity of the ABCG2-Y413S mutant showed a sterol sensitivity that significantly differed from that of the wild-type, while in the vesicular transport measurement the effect of cholesterol on this mutant did not differ from that measured for wtABCG2. In order to further characterize the "cholesterol-dependence" of the CRAC mutant ABCG2 proteins, we generated mammalian HEK 293 cells stably expressing the Y413S, Y469F, Y570S and Y645F mutants. Western blotting confirmed successful expression of these proteins (data not shown). Moreover, labeling with the anti-ABCG2 5D3 antibody, which recognizes an extracellular epitope, indicated proper plasma membrane localization of these mutants (Supplementary Fig. S2).

To characterize the effect of cholesterol on the ABCG2 transport function, we depleted the cholesterol content of the cells by co-incubation with cyclodextrin (RAMEB). This method decreases membrane cholesterol levels by about 25%, and was successfully used in earlier studies to define the effects of various cholesterol levels on ABCG2 function in mammalian cells [15, 33]. Previously we have demonstrated that mild cholesterol depletion of HEK 293 cells resulted in a decreased transport function of wtABCG2, while did not alter the localization of ABCG2 or the viability of the cells [15].

For measuring ABCG2 transport activity, intracellular accumulation of Hoechst 33342 was followed in control and cyclodextrin-treated HEK 293 cells, expressing the wild-type and the CRAC mutant ABCG2 variants. As shown in Fig. 7, all ABCG2 mutants, including Y413S,

were able to actively transport Hoechst 33342, and cholesterol depletion significantly decreased the Hoechst 33342 transport activity of all the CRAC mutants similarly to wild-type ABCG2.

3.7. Putative CRAC mutants of ABCG2, including Y413S, effectively transport substrate drugs and protect HEK 293 cells against cytotoxic substrates

The differential effects of the transported substrates on the wild-type and the Y413S ABCG2 ATPase activity may reflect different transport properties. Still, we did not find any alteration of the transport capacity or the cholesterol sensitivity of the Hoechst 33342 transport in the CRAC mutants.

In order to further explore the relationship of altered drug-stimulated ATPase and transport activities, the transport of various fluorescent ABCG2 substrates was compared in HEK 293 cells overexpressing wtABCG2 and the Y413S mutant, respectively. No major difference was found in BODIPY-prazosin, Hoechst 33342, mitoxantrone and Pheophorbide A transport by any of the active mutants analyzed in this study (Table I). Interestingly, in spite of its different behavior in the ATPase assay, the Y413S mutant also did not differ significantly from the wild-type protein, with respect to the transport of the above mentioned substrates.

Among the cytotoxic drugs, the Y413S mutant ABCG2 protein (similarly to the wild-type) was able to transport doxorubicin (Fig. 8A) and provided protection against doxorubicin, SN-38, flavopiridol and topotecan, strongly indicating an active transport of these compounds by this mutant (Fig. 8B and Supplementary Fig. S3).

4. Discussion

Understanding the regulation of the expression and function of ABCG2 may have important implications with regard to the modulation the ADME-Tox parameters of drugs and xenobiotics, in anti-cancer therapies, as well as in the treatment of gout. Cholesterol has been shown to be an essential activator of ABCG2 function [14-16], although the exact nature of the interaction between cholesterol and the transporter has not yet been defined. Also, the molecular determinants of cholesterol sensing by ABCG2 remain largely unknown [19, 20]. Cholesterol recognition amino acid consensus sequence (CRAC) motifs have previously been confirmed to be involved in cholesterol sensing of various proteins [21-25, 34, 35]. Site directed mutagenesis studies targeting conserved CRAC amino acids identified a large variety of protein-specific phenotypes. In the case of the HIV gp41 protein, CRAC mutations resulted in reduced cholesterol binding [35]; mutant peripheral-type benzodiazepine receptor variants showed altered cholesterol transport [34], while in ion channels the channel function was retained but regulation by cholesterol was abolished [25, 36].

Here, we aimed to determine whether the CRAC motifs identified in the ABCG2 sequence play any role in the sterol sensing of the human ABCG2 multidrug transporter. We found five putative CRAC sequences located in or near the transmembrane helices of ABCG2 (Fig. 1). Based on the previous CRAC mutagenesis studies described above, we expected that mutation of a functional CRAC motif would modify the effect of cholesterol on ABCG2 function. We have approached this question by using a number of specific methods.

ABC transporters couple ATPase and transport activities to promote the transmembrane movement of their substrates. This complex enzymatic activity can be followed in several experimental systems. ABCG2 expressed in Sf9 membranes displays relatively high baseline ATPase activity that can be moderately stimulated by transported compounds. The low intrinsic cholesterol content of the insect cell membrane allows the systematic modulation of membrane cholesterol levels. Using this model system, we and others have shown that the substrate-stimulated ATPase activity of ABCG2 is significantly accelerated by cholesterol [14, 15]. Cholesterol makes up to 20% of the total lipids in mammalian cell membranes. Partial cholesterol depletion can be achieved by using “empty” cyclodextrins, which has been shown to result in a decrease of ABCG2 transport activity [15, 33]. Using this repertoire of assays we aimed to determine the role of the identified five CRAC motifs in the cholesterol-sensitive functions of ABCG2.

We found that tyrosines of putative CRAC motifs predicted to be located in or near to the intracellular surface of ABCG2 (Fig. 1) are essential for protein expression and/or function. Tyr to Ser mutations at positions 459, 469 and 645 resulted in the loss of protein function, and the Tyr 459 to Ser mutation resulted in a complete loss of ABCG2 expression (Fig. 2). Insect cells are cultured at 27ºC which has been shown to allow the expression of improperly folded proteins [37]. The fact that the Y459S mutant could not be expressed properly in insect cells suggests that the tyrosine at this amino acid position is crucial for the proper folding and processing of the protein and therefore might be an important determinant of ABCG2 structure. Recently, the Y459C heterozygous mutation was reported to occur in patients with renal cancer [38]. Therefore further exploration of the effect of mutations to residue 459 in ABCG2 is warranted.

The Y469S and Y645S mutants could be expressed in comparable amounts to the wild-type protein, however, they were found to be non-functional (Fig. 2). These results may be interpreted in two ways. First, these tyrosines may be important for proper function or, alternatively, these mutants may lose their cholesterol sensing capability. Interestingly, introduction of a phenyl residue at the same position was found to be compatible with normal ATPase and transport activity, as well as with cholesterol sensing, indicating that these regions are not functional CRAC motifs. Rather, Y469 and Y645, along with Y459, may be important for proper folding of ABCG2. Our experiments, in which we tested the conformation of the ABCG2 mutants by labeling them with the conformation sensitive anti-ABCG2 5D3 antibody, revealed that the Y469S and Y645S mutants have decreased 5D3 binding capacity (Supplementary Figure S4). Therefore the loss of the activity of the Y469S and Y645S mutants is most probably due to their improper conformation and not by their altered cholesterol sensing.

Previously, the Y645F mutation has been found to be functional, although has shown slightly decreased Hoechst 33342 transport capacity [39]. Interestingly, we did not find any major alteration in the substrate recognition by this mutant. Even its Hoechst 33342 transport capacity did not differ significantly from that of the wild-type protein (Fig. 7).

The other two tyrosines (Y413 and Y570) mutated in this study are located in or near the extracellular surface of the transmembrane domain. We found that changing these amino acids is well tolerable for ABCG2, resulting in fully active proteins. The Tyr 570 to Ser mutation did not alter protein expression either in Sf9 or in HEK 293 cells, and substrate recognition and cholesterol-sensing of this mutant was also similar to that of the wild-type transporter (Fig. 2 and 6 and Supplementary Fig. S1).

However, the Y413S mutant exhibited a distinct ATPase activity. This mutant showed a greatly increased baseline ATPase in the presence of low levels of added cholesterol (Fig. 4A), revealing an increased cholesterol sensitivity, while no further activation of the ABCG2-413S ATPase could be achieved by administration of transported substrates regardless of the cholesterol content of the membrane. Moreover, potential substrates that are known to activate the wild-type ABCG2-ATPase, rather inhibited the ATPase activity of the Y413S mutant (Fig. 3). In addition to this altered cholesterol-sensing, the ATPase activity of the Y413S mutant also had an altered bile acid sensitivity, as this mutant was less sensitive to bile acids than the wild-type protein (Fig. 5).

The nature of the relatively high baseline ATPase activity of the human ABCG2 transporter is still not clarified. One explanation is an intrinsic, partially uncoupled function of the protein, manifesting in a "futile" ATP hydrolysis, keeping this multidrug transporter alert for rapid export of potentially harmful compounds [40]. Another possibility is the presence of an endogenous transported substrate, potentially cholesterol, triggering ATP hydrolysis without the addition of exogenous compounds. In the case of the Y413S mutant, cholesterol may promote "uncoupling" of the ATP hydrolysis in the ABCG2 protein. Alternatively, if we consider the possibility that cholesterol is transported by ABCG2, the results could be explained by a higher affinity to cholesterol by the ABCG2-Y413S mutant, also observed in the case of the R482G mutant [15]. The cholesterol-dependent increase in the ATPase activity is similar to that observed for several transported substrates. If ABCG2 can transport cholesterol, our data can be interpreted to suggest that the Y413S mutant is a more efficient cholesterol transporter. Unfortunately, experimental verification of cholesterol transport is difficult due to the lack of dedicated assays measuring ABCG2-mediated cholesterol transport. Tarling et al. [41] measured cholesterol efflux to HDL in ABCG1 and ABCG2 overexpressing cells, and found that, in contrast to ABCG1, ABCG2 is not able to transport cholesterol to HDL. Since ABCG2-mediated cholesterol transport has not been experimentally confirmed, we speculate that the "cholesterol-stimulated" ATPase activity of the ABCG2-Y413S mutant is a result of its differential sensitivity to the modulatory effect of cholesterol.

In contrast to these findings related to the ABCG2-ATPase activity, we did not find any significant alteration in the cholesterol sensitivity of the ABCG2-Y413S mediated transport either in insect cell vesicular transport, or mammalian whole cell transport assays. Active substrate transport by the Y413S mutant was clearly activated by cholesterol in both systems, and by all the compounds examined (Fig. 6 and 7). Moreover, the Y413S mutant protected the cells against toxic drugs similarly to the wild-type ABCG2. All these experimental data suggest

that although the ABCG2-Y413S mutant has an altered cholesterol interaction, it is rather manifested in a partial uncoupling of the ATPase activity of the transporter in the absence of transported substrates.

5. Conclusions

Our study is the first detailed analysis of potential CRAC motifs within an ABC protein, and here we provide experimental data for various functional consequences of the mutations in these motifs in ABCG2. Surprisingly, none of the functional mutants, containing putative CRAC motifs analyzed here abolished the cholesterol-sensitivity of the transporter, although mutation of Y413 significantly affected cholesterol and bile acid interactions. These data suggest that Tyr 413 within a putative CRAC motif is most probably part of a sterol-dependent regulatory region of ABCG2 and may regulate the coupling of ATPase to transport activity.

Acknowledgements

We are grateful to Hedvig Tordai for providing us the pSB-CMV-ABCG2 plasmid and to György Várady for helping in cell sorting. The technical help by Zsuzsanna Andrási, Éva Krizsán, Katalin Mihály and Györgyi Vermes is also greatly appreciated. We are also thankful to Drs. George Scheffer and Rik Scheper for providing us the BXP-21 antibody (Department of Pathology, Free University, Medical Center, Amsterdam, the Netherlands).

Funding: This work has been supported by the Hungarian Scientific Research Fund (OTKA) grants [83533, 109423 and 104227], and by NKTH-ANR [10-1-2011-0401] Achilles. G. Sz. was supported by a Momentum Grant of the Hungarian Academy of Sciences.

References

[1] B. Sarkadi, C. Ozvegy-Laczka, K. Nemet, A. Varadi, ABCG2 -- a transporter for all seasons, FEBS Lett, 567 (2004) 116-120.
[2] U. Henriksen, J.U. Fog, T. Litman, U. Gether, Identification of intra- and intermolecular disulfide bridges in the multidrug resistance transporter ABCG2, J Biol Chem, 280 (2005) 36926-36934.
[3] K. Noguchi, K. Katayama, Y. Sugimoto, Human ABC transporter ABCG2/BCRP expression in chemoresistance: basic and clinical perspectives for molecular cancer therapeutics, Pharmacogenomics and personalized medicine, 7 (2014) 53-64.
[4] I.D. Kerr, A.J. Haider, I.C. Gelissen, The ABCG family of membrane-associated transporters: you don't have to be big to be mighty, Br J Pharmacol, 164 (2011) 1767-1779.
[5] G. Szakacs, A. Varadi, C. Ozvegy-Laczka, B. Sarkadi, The role of ABC transporters in drug absorption, distribution, metabolism, excretion and toxicity (ADME-Tox), Drug discovery today, 13 (2008) 379-393.
[6] P. Godoy, N.J. Hewitt, U. Albrecht, M.E. Andersen, N. Ansari, S. Bhattacharya, J.G. Bode, J. Bolleyn, C. Borner, J. Bottger, A. Braeuning, R.A. Budinsky, B. Burkhardt, N.R. Cameron, G. Camussi, C.S. Cho, Y.J. Choi, J. Craig Rowlands, U. Dahmen, G. Damm, O. Dirsch, M.T. Donato, J. Dong, S. Dooley, D. Drasdo, R. Eakins, K.S. Ferreira, V. Fonsato, J. Fraczek, R. Gebhardt, A. Gibson, M. Glanemann, C.E. Goldring, M.J. Gomez-Lechon, G.M. Groothuis, L. Gustavsson, C. Guyot, D. Hallifax, S. Hammad, A. Hayward, D. Haussinger, C. Hellerbrand, P. Hewitt, S. Hoehme, H.G. Holzhutter, J.B. Houston, J. Hrach, K. Ito, H. Jaeschke, V. Keitel, J.M. Kelm, B. Kevin Park, C. Kordes, G.A. Kullak-Ublick, E.L. LeCluyse, P. Lu, J. Luebke-Wheeler, A. Lutz, D.J. Maltman, M. Matz-Soja, P. McMullen, I. Merfort, S. Messner, C. Meyer, J. Mwinyi, D.J. Naisbitt, A.K. Nussler, P. Olinga, F. Pampaloni, J. Pi, L. Pluta, S.A. Przyborski, A. Ramachandran, V. Rogiers, C. Rowe, C. Schelcher, K. Schmich, M. Schwarz, B. Singh, E.H. Stelzer, B. Stieger, R. Stober, Y. Sugiyama, C. Tetta, W.E. Thasler, T. Vanhaecke, M. Vinken, T.S. Weiss, A. Widera, C.G. Woods, J.J. Xu, K.M. Yarborough, J.G. Hengstler, Recent advances in 2D and 3D in vitro systems using primary hepatocytes, alternative hepatocyte sources and non-parenchymal liver cells and their use in investigating mechanisms of hepatotoxicity, cell signaling and ADME, Archives of toxicology, 87 (2013) 1315-1530.
[7] O.M. Woodward, A. Kottgen, J. Coresh, E. Boerwinkle, W.B. Guggino, M. Kottgen, Identification of a urate transporter, ABCG2, with a common functional polymorphism causing gout, Proc Natl Acad Sci U S A, 106 (2009) 10338-10342.
[8] A. Nakayama, H. Matsuo, T. Takada, K. Ichida, T. Nakamura, Y. Ikebuchi, K. Ito, T. Hosoya, Y. Kanai, H. Suzuki, N. Shinomiya, ABCG2 is a high-capacity urate transporter and its genetic impairment increases serum uric acid levels in humans, Nucleosides Nucleotides Nucleic Acids, 30 (2011) 1091-1097.
[9] A. Dehghan, A. Kottgen, Q. Yang, S.J. Hwang, W.L. Kao, F. Rivadeneira, E. Boerwinkle, D. Levy, A. Hofman, B.C. Astor, E.J. Benjamin, C.M. van Duijn, J.C. Witteman, J. Coresh, C.S. Fox, Association of three genetic loci with uric acid concentration and risk of gout: a genome-wide association study, Lancet, 372 (2008) 1953-1961.
[10] P. Krishnamurthy, J.D. Schuetz, The ABC transporter Abcg2/Bcrp: role in hypoxia mediated survival, Biometals, 18 (2005) 349-358.
[11] D. Turk, G. Szakacs, Relevance of multidrug resistance in the age of targeted therapy, Current opinion in drug discovery & development, 12 (2009) 246-252.
[12] R.W. Robey, P.R. Massey, L. Amiri-Kordestani, S.E. Bates, ABC transporters: unvalidated therapeutic targets in cancer and the CNS, Anticancer Agents Med Chem, 10 (2010) 625-633.

[13] K. Natarajan, Y. Xie, M.R. Baer, D.D. Ross, Role of breast cancer resistance protein (BCRP/ABCG2) in cancer drug resistance, Biochem Pharmacol, 83 (2012) 1084-1103.
[14] A. Pal, D. Mehn, E. Molnar, S. Gedey, P. Meszaros, T. Nagy, H. Glavinas, T. Janaky, O. von Richter, G. Bathori, L. Szente, P. Krajcsi, Cholesterol potentiates ABCG2 activity in a heterologous expression system: improved in vitro model to study function of human ABCG2, J Pharmacol Exp Ther, 321 (2007) 1085-1094.
[15] A. Telbisz, C. Hegedus, A. Varadi, B. Sarkadi, C. Ozvegy-Laczka, Regulation of the Function of the Human ABCG2 Multidrug Transporter by Cholesterol and Bile Acids: Effects of Mutations in Potential Substrate and Steroid Binding Sites, Drug Metab Dispos, 42 (2007) 575-585.
[16] A. Telbisz, C. Ozvegy-Laczka, T. Hegedus, A. Varadi, B. Sarkadi, Effects of the lipid environment, cholesterol and bile acids on the function of the purified and reconstituted human ABCG2 protein, Biochem J, 450 (2013) 387-395.
[17] G.A. Graf, L. Yu, W.P. Li, R. Gerard, P.L. Tuma, J.C. Cohen, H.H. Hobbs, ABCG5 and ABCG8 are obligate heterodimers for protein trafficking and biliary cholesterol excretion, J Biol Chem, 278 (2003) 48275-48282.
[18] N. Wang, L. Yvan-Charvet, D. Lutjohann, M. Mulder, T. Vanmierlo, T.W. Kim, A.R. Tall, ATP-binding cassette transporters G1 and G4 mediate cholesterol and desmosterol efflux to HDL and regulate sterol accumulation in the brain, FASEB J, 22 (2008) 1073-1082.
[19] A. Telbisz, C. Hegedus, A. Varadi, B. Sarkadi, C. Ozvegy-Laczka, Regulation of the function of the human ABCG2 multidrug transporter by cholesterol and bile acids: effects of mutations in potential substrate and steroid binding sites, Drug Metab Dispos, 42 (2014) 575-585.
[20] S. Velamakanni, T. Janvilisri, S. Shahi, H.W. van Veen, A functional steroid-binding element in an ATP-binding cassette multidrug transporter, Mol Pharmacol, 73 (2008) 12-17.
[21] J.J. Lacapere, V. Papadopoulos, Peripheral-type benzodiazepine receptor: structure and function of a cholesterol-binding protein in steroid and bile acid biosynthesis, Steroids, 68 (2003) 569-585.
[22] R.M. Epand, Proteins and cholesterol-rich domains, Biochim Biophys Acta, 1778 (2008) 1576-1582.
[23] R.M. Epand, B.G. Sayer, R.F. Epand, Caveolin scaffolding region and cholesterol-rich domains in membranes, J Mol Biol, 345 (2005) 339-350.
[24] A. Midzak, G. Rammouz, V. Papadopoulos, Structure-activity relationship (SAR) analysis of a family of steroids acutely controlling steroidogenesis, Steroids, 77 (2012) 1327-1334.
[25] A.K. Singh, J. McMillan, A.N. Bukiya, B. Burton, A.L. Parrill, A.M. Dopico, Multiple cholesterol recognition/interaction amino acid consensus (CRAC) motifs in cytosolic C tail of Slo1 subunit determine cholesterol sensitivity of Ca2+- and voltage-gated K+ (BK) channels, J Biol Chem, 287 (2012) 20509-20521.
[26] C. Ozvegy, A. Varadi, B. Sarkadi, Characterization of drug transport, ATP hydrolysis, and nucleotide trapping by the human ABCG2 multidrug transporter. Modulation of substrate specificity by a point mutation, J Biol Chem, 277 (2002) 47980-47990.
[27] C. Ozvegy, T. Litman, G. Szakacs, Z. Nagy, S. Bates, A. Varadi, B. Sarkadi, Functional characterization of the human multidrug transporter, ABCG2, expressed in insect cells, Biochem Biophys Res Commun, 285 (2001) 111-117.
[28] H. Saranko, H. Tordai, A. Telbisz, C. Ozvegy-Laczka, G. Erdos, B. Sarkadi, T. Hegedus, Effects of the gout-causing Q141K polymorphism and a CFTR DeltaF508 mimicking mutation on the processing and stability of the ABCG2 protein, Biochem Biophys Res Commun, 437 (2013) 140-145.

[29] O. Kolacsek, V. Krizsik, A. Schamberger, Z. Erdei, A. Apati, G. Varady, L. Mates, Z. Izsvak, Z. Ivics, B. Sarkadi, T.I. Orban, Reliable transgene-independent method for determining Sleeping Beauty transposon copy numbers, Mob DNA, 2 (2011) 5.
[30] E. Bakos, I. Klein, E. Welker, K. Szabo, M. Muller, B. Sarkadi, A. Varadi, Characterization of the human multidrug resistance protein containing mutations in the ATP-binding cassette signature region, Biochem J, 323 (Pt 3) (1997) 777-783.
[31] M.F. Khan, Unruh, T. L., and Deans, J. P., Implementation of a Flow Cytometry Strategy to
Isolate and Assess Heterogeneous Membrane Raft Domains, Flow Cytometry - Recent Perspectives, (2012).
[32] C. Ozvegy-Laczka, G. Koblos, B. Sarkadi, A. Varadi, Single amino acid (482) variants of the ABCG2 multidrug transporter: major differences in transport capacity and substrate recognition, Biochim Biophys Acta, 1668 (2005) 53-63.
[33] C.H. Storch, R. Ehehalt, W.E. Haefeli, J. Weiss, Localization of the human breast cancer resistance protein (BCRP/ABCG2) in lipid rafts/caveolae and modulation of its activity by cholesterol in vitro, J Pharmacol Exp Ther, 323 (2007) 257-264.
[34] H. Li, V. Papadopoulos, Peripheral-type benzodiazepine receptor function in cholesterol transport. Identification of a putative cholesterol recognition/interaction amino acid sequence and consensus pattern, Endocrinology, 139 (1998) 4991-4997.
[35] R.F. Epand, B.G. Sayer, R.M. Epand, The tryptophan-rich region of HIV gp41 and the promotion of cholesterol-rich domains, Biochemistry, 44 (2005) 5525-5531.
[36] S. Oddi, E. Dainese, F. Fezza, M. Lanuti, D. Barcaroli, V. De Laurenzi, D. Centonze, M. Maccarrone, Functional characterization of putative cholesterol binding sequence (CRAC) in human type-1 cannabinoid receptor, Journal of neurochemistry, 116 (2011) 858-865.
[37] G.M. Denning, M.P. Anderson, J.F. Amara, J. Marshall, A.E. Smith, M.J. Welsh, Processing of mutant cystic fibrosis transmembrane conductance regulator is temperature-sensitive, Nature, 358 (1992) 761-764.
[38] I. Zoernig, C. Ziegelmeier, B. Lahrmann, N. Grabe, D. Jager, N. Halama, Sequence mutations of the substrate binding pocket of stem cell factor and multidrug resistance protein ABCG2 in renal cell cancer: a possible link to treatment resistance, Oncol Rep, 29 (2013) 1697-1700.
[39] Z. Ni, Z. Bikadi, X. Cai, M.F. Rosenberg, Q. Mao, Transmembrane helices 1 and 6 of the human breast cancer resistance protein (BCRP/ABCG2): identification of polar residues important for drug transport, Am J Physiol Cell Physiol, 299 (2010) C1100-1109.
[40] B. Sarkadi, L. Homolya, G. Szakacs, A. Varadi, Human multidrug resistance ABCB and ABCG transporters: participation in a chemoimmunity defense system, Physiological reviews, 86 (2006) 1179-1236.
[41] E.J. Tarling, P.A. Edwards, ATP binding cassette transporter G1 (ABCG1) is an intracellular sterol transporter, Proc Natl Acad Sci U S A, 108 (2011) 19719-19724.
[42] G.E. Tusnady, I. Simon, The HMMTOP transmembrane topology prediction server, Bioinformatics, 17 (2001) 849-850.
[43] L. Dobson, Reményi, I., and Tusnády, G. E. , The Human Transmembrane Proteome submitted to Plos One, (2014).

FIGURE LEGENDS

Figure 1. Topology model of human ABCG2 indicating the positions of tyrosines mutated in this study and also showing sequence alignment of human ABCG proteins. Protein sequences of human ABCG proteins (ABCG2 AAG52982.1, ABCG1 P45844.3, ABCG4 NP_001135977.1, ABCG5 AG40003.1, ABCG8 AAG40004.1) were aligned using Clustalw (https://www.ebi.ac.uk/Tools/msa/clustalw2/). Putative CRAC motifs are underlined; the 3 conserved amino acids in CRAC motifs are labeled with bold letters. The 2D structure was drawn by using http://emboss.bioinformatics.nl/cgi-bin/emboss/topo based on the topology created by CCTOP (http://htp.enzim.hu/?_=/viewer/HTP_002649) [42, 43].

Figure 2. Expression and ATPase activity of ABCG2 CRAC tyrosine mutants in Sf9 insect cells. Panel A: Expression of CRAC mutants in Sf9 membranes. Sf9 membranes expressing wtABCG2 and its Tyr mutants were subjected to Laemmli gel electrophoresis. ABCG2 was visualized by the BXP-21 antibody. **Panel B-C: ATPase activity of ABCG2-CRAC mutants in Sf9 insect membranes.** Vanadate-sensitive ATPase activity was measured in non-treated (labeled as control, Panel B) insect membranes or in membranes loaded with 2 mM cholesterol-RAMEB (Panel C) during the membrane preparation (see 2.6.) in the absence of added compounds (baseline), or in the presence of 1 μM quercetin, 100 μM prazosin or 1 μM Ko143. Bars show the average of at least two independent experiments, each with two parallels, +/- S.D. values.

Figure 3. Effect of known wtABCG2 substrates on the ATPase activity of wtABCG2 and the Y413S mutant. Vanadate-sensitive ATPase activity was determined in 2 mM cholesterol-RAMEB treated membranes in the absence of substrates (baseline) or in the presence of 5 μM quercetin, 50 μM doxorubicin, 20 μM SN-38, 50 μM flavopiridol or 50 μM topotecan (Panels A and B). ATPase activity was also determined in the presence of increasing concentrations of doxorubicin or topotecan (Panels C and D). Figure shows the result of three independent experiments, +/- S.D. values.

Figure 4. Effect of cholesterol on the wtABCG2 and Y413S-ATPase. Vanadate-sensitive ATPase activity was determined as described in 2.9. Control membranes were co-incubated with 0.25-2 mM cholesterol-RAMEB to achieve various membrane cholesterol levels. ATPase activity was measured in the absence of added substrates (Panel A) or in the presence of 5 μM

quercetin (Panel B). The average of four independent experiments +/- S.D. values are shown. *: Student's t-test, significant difference, $p < 0.05$.

Figure 5: **Effect of bile acids on the wtABCG2 and Y413S-ATPase.** ATPase activity was determined in Sf9 membrane vesicles loaded with 2 mM cholesterol-RAMEB. **Panel A**: Vanadate-sensitive basal (no added substrate) or 1 μM quercetin-stimulated ATPase activity in the absence or presence of 1 mM glycocholate (GC), 1 mM cholic acid (CA) or taurocholate (TC). **Panel B**: Relative ATPase activity in the presence of 1 μM quercetin compared to the baseline is shown against increasing bile acid concentrations. Experiments were performed in quadruplicates, average +/- S.D. values are shown.

Figure 6. Transport of ^{3}H-methotrexate into control and cholesterol-loaded inside-out Sf9 insect membrane vesicles. Intravesicular accumulation of 50 μM ^{3}H-methotrexate in Sf9 membrane vesicles with different ABCG2 mutants containing 90 μg of total membrane protein was measured at 37^{o}C for 10 minutes in the presence or absence of 1 μM Ko143. For the investigation of the effect of cholesterol, the membranes were loaded with 2 mM cholesterol-RAMEB. Control represents non-loaded membranes. Bars represent average Ko143-dependent transport obtained in two independent experiments, each with two parallels +/- S.D. values.

Figure 7. Hoechst 33342 transport in ABCG2-expressing HEK 293 cells - effect of cholesterol depletion. HEK 293 cells stably expressing wtABCG2 and its mutants were incubated with 2 μM Hoechst 33342 for 20 minutes at 37^{o}C with or without 1 μM Ko143. After washing, cellular fluorescence of Hoechst 33342 was determined by flow cytometry. Cholesterol depletion was achieved by co-incubation of the membranes with empty cyclodextrin (see 2.12.); control values show results obtained with non-treated cells. Transport factor in living (propidium-iodide negative) cells was calculated as described in 2.11. Experiments were performed in quadruplicates; bars show the average of at least three independent measurements +/- S.D. values.

Figure 8. Panel A: Doxorubicin efflux from HEK 293 cells. Doxorubicin (5 μM) efflux was measured as described in 2.13. Fluorescence of the cells was monitored by flow cytometry. Experiments were performed in duplicates. Figure shows representative graphs. **Panel B. Cytotoxicy of ABCG2 substrates in HEK 293 cells.** HEK 293 parental cells or stably

expressing wtABCG2 or its Y413S mutant were incubated with 50 nM SN-38, 50 nM topotecan (TOP), 60 nM doxorubicin (DOX) or 500 nM flavopiridol (FLP) for 72 hours. Cell viability was determined by PrestoBlue staining. 100% represents cells incubated at the same conditions in the absence of any drugs. Bars show the average of four independent experiments with quadruplicates each, +/- S.D. values.

Figure 1

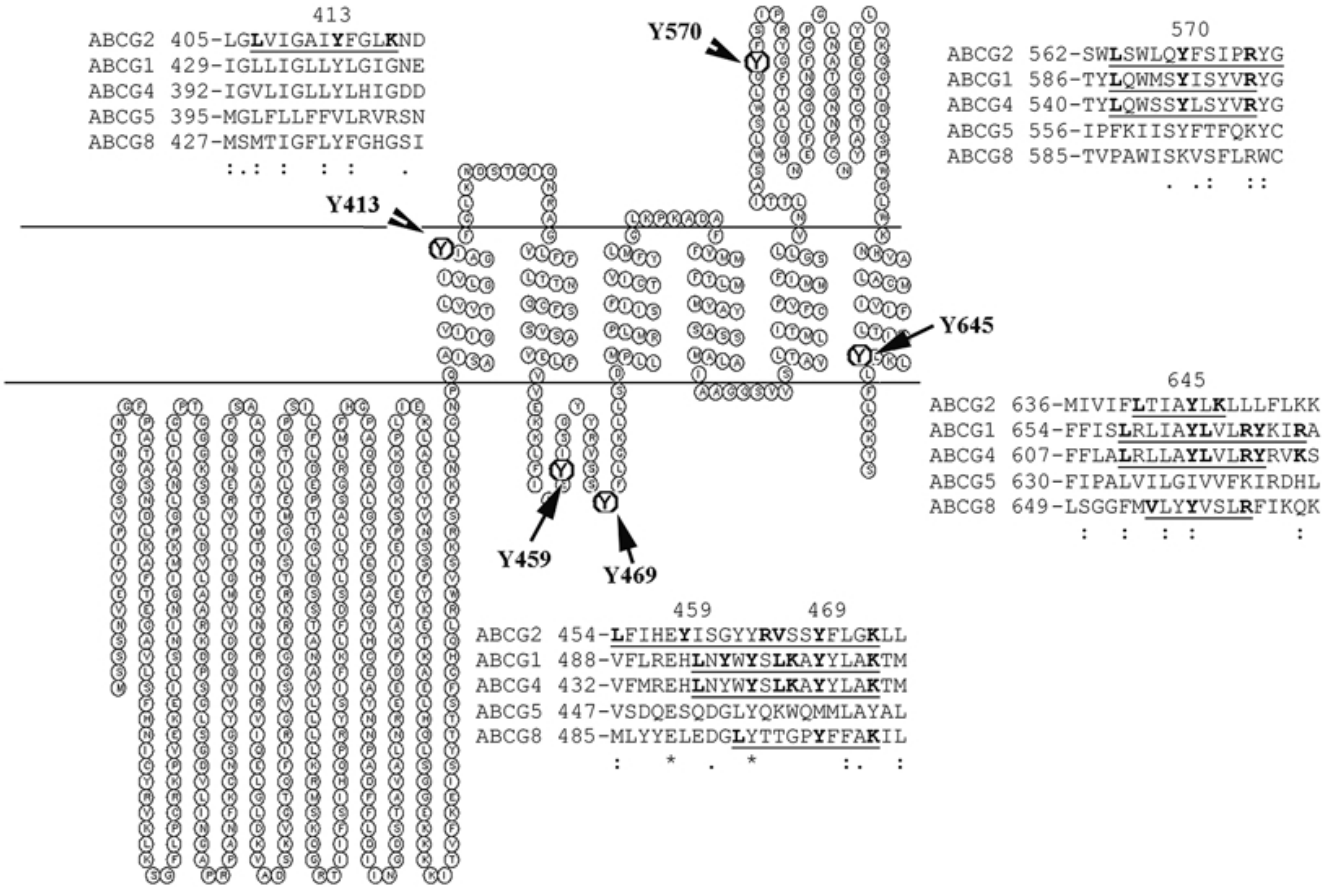
413
ABCG2 405-LGLVIGAIYFGLKND
ABCG1 429-IGLLIGLLYLGIGNE
ABCG4 392-IGVLIGLLYLHIGDD
ABCG5 395-MGLFLLFFVLRVRSN
ABCG8 427-MSMTIGFLYFGHGSI
Y413
Y570
570
ABCG2 562-SWLSWLQYFSIPRYG
ABCG1 586-TYLQWMSYISYVRYG
ABCG4 540-TYLQWSSYLSYVRYG
ABCG5 556-IPFKIISYFTFQKYC
ABCG8 585-TVPAWISKVSFLRWC
Y645
645
ABCG2 636-MIVIFLTIAYLKLLLFLKK
ABCG1 654-FFISLRLIAYLVLRYKIRA
ABCG4 607-FFLALRLLAYLVLRYRVKS
ABCG5 630-FIPALVILGIVVFKIRDHL
ABCG8 649-LSGGFMVLYYVSLRFIKQK
Y459
Y469
459
469
ABCG2 454-LFIHEYISGYYRVSSYFLGKLL
ABCG1 488-VFLREHLNYWYSLKAYYLAKTM
ABCG4 432-VFMREHLNYWYSLKAYYLAKTM
ABCG5 447-VSDQESQDGLYQKWQMMLAYAL
ABCG8 485-MLYYELEDGLYTTGPYFFAKIL

Figure 2

A

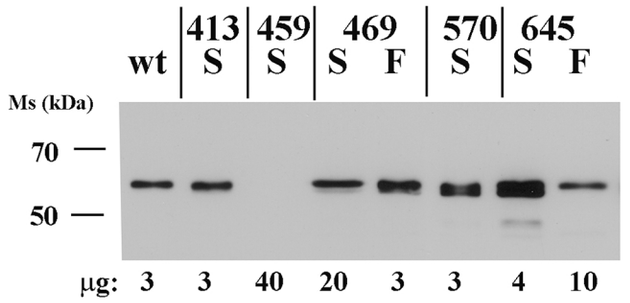
wt
413 S
459 S
469 S F
570 S
645 S F
Ms (kDa)
70
50
μg: 3 3 40 20 3 3 4 10

B

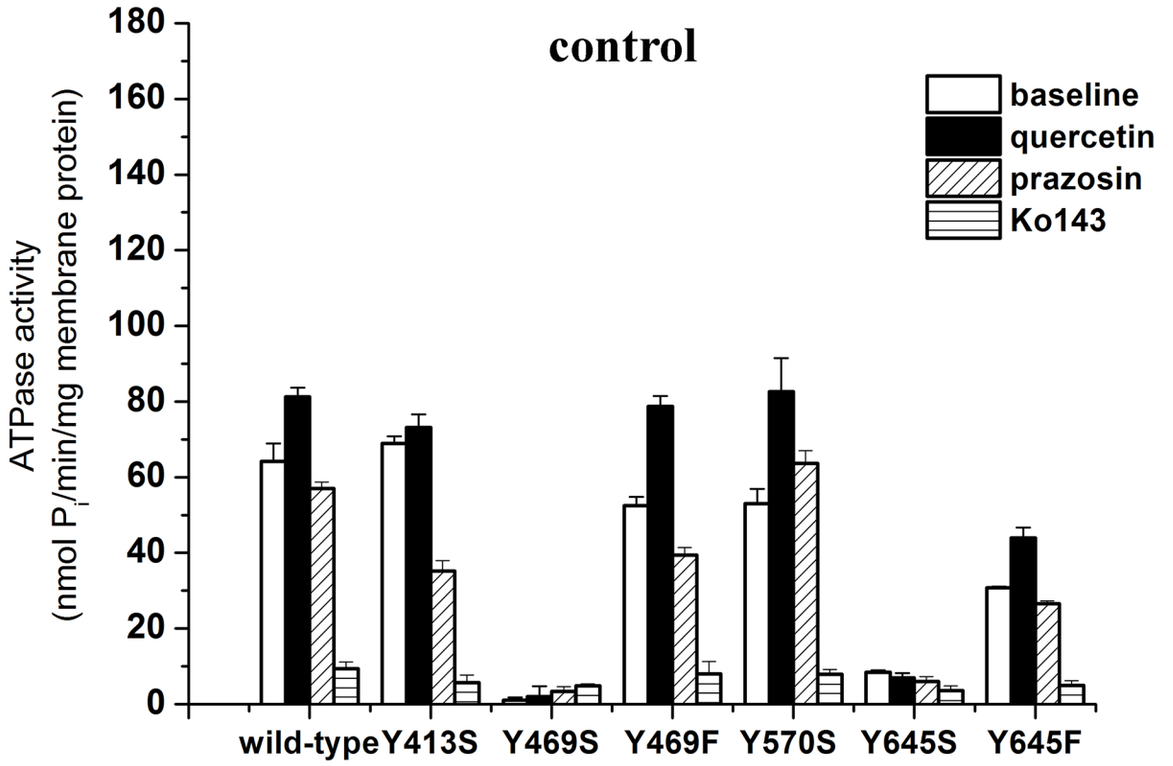
control
baseline
quercetin
prazosin
Ko143
ATPase activity
(nmol P_i/min/mg membrane protein)
0
20
40
60
80
100
120
140
160
180
wild-type
Y413S
Y469S
Y469F
Y570S
Y645S
Y645F

C

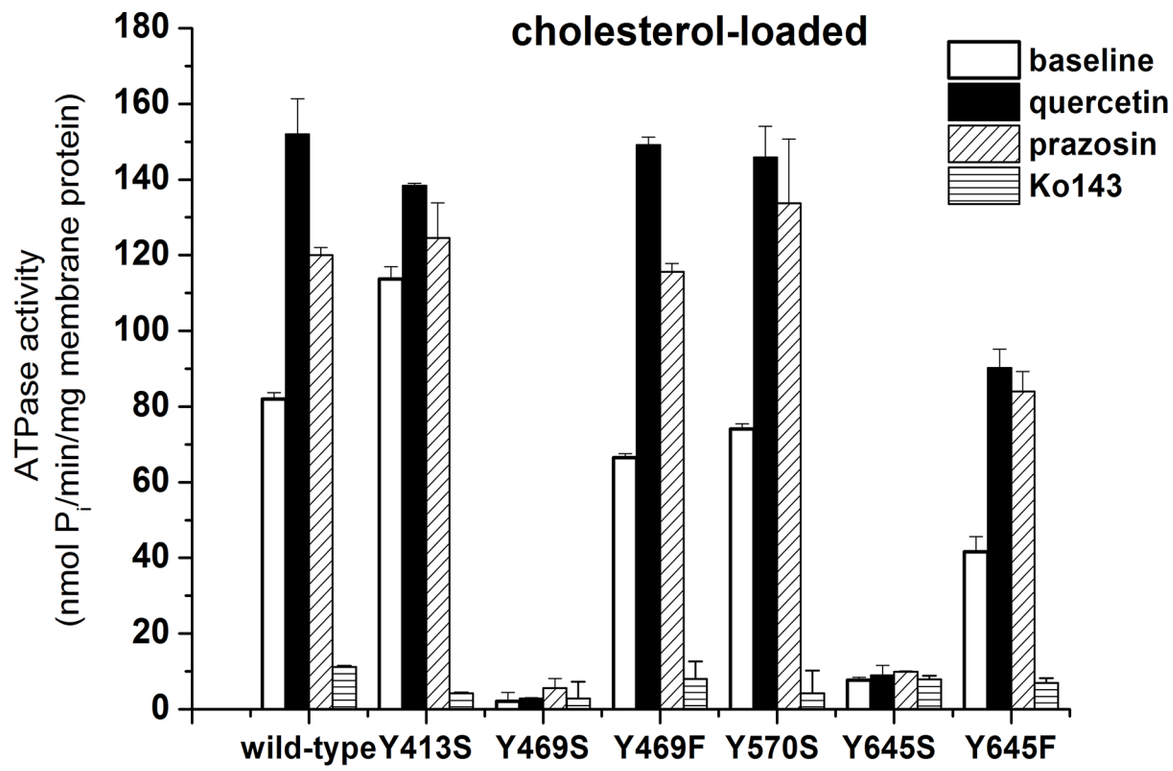
cholesterol-loaded
baseline
quercetin
prazosin
Ko143
ATPase activity
(nmol P_i/min/mg membrane protein)
0
20
40
60
80
100
120
140
160
180
wild-type
Y413S
Y469S
Y469F
Y570S
Y645S
Y645F

Figure 3

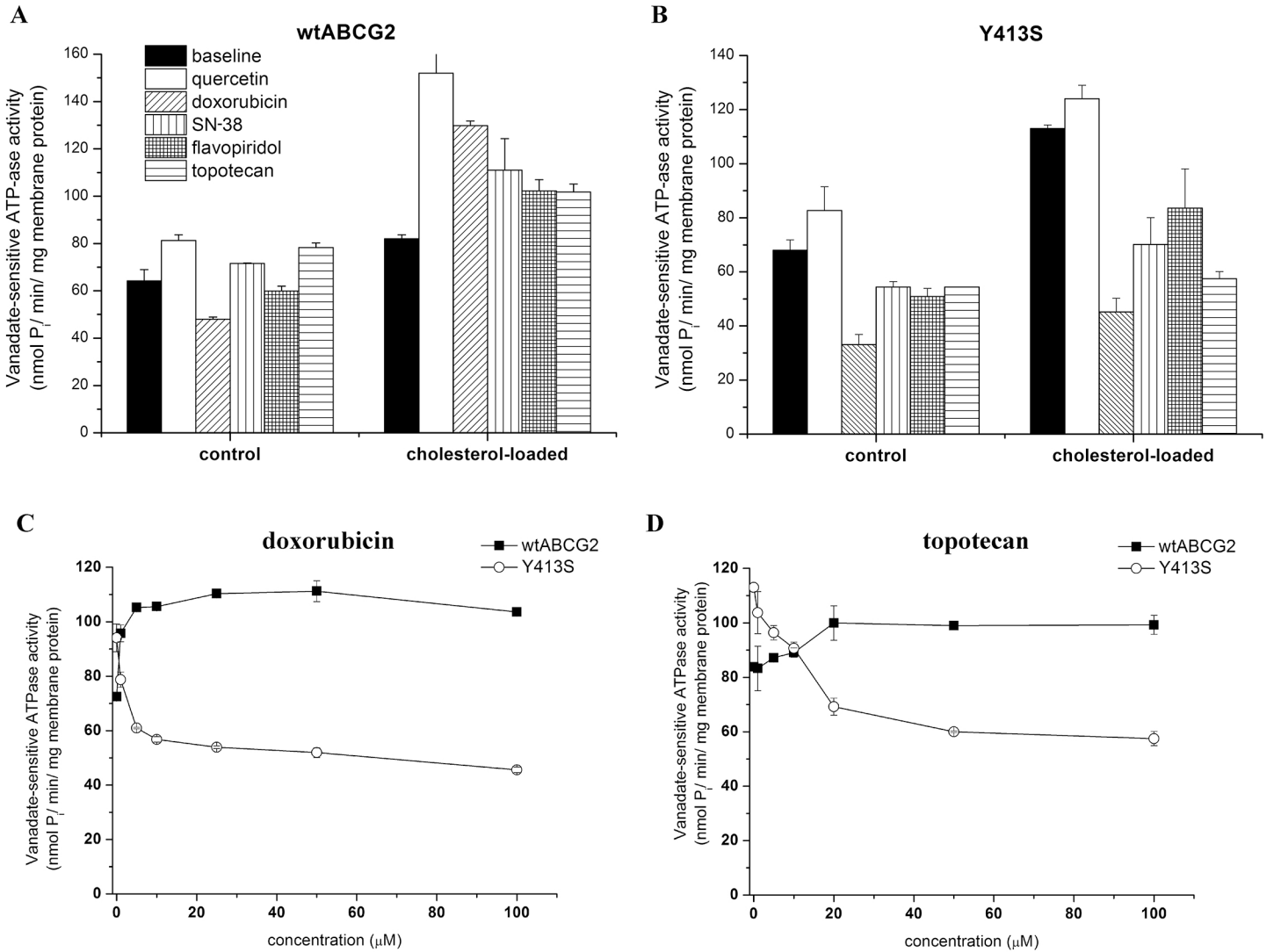
A
wtABCG2
baseline
quercetin
doxorubicin
SN-38
flavopiridol
topotecan
Vanadate-sensitive ATP-ase activity
(nmol P$_i$/ min/ mg membrane protein)
control
cholesterol-loaded
B
Y413S
Vanadate-sensitive ATP-ase activity
(nmol P$_i$/ min/ mg membrane protein)
control
cholesterol-loaded
C
doxorubicin
wtABCG2
Y413S
Vanadate-sensitive ATPase activity
(nmol P$_i$/ min/ mg membrane protein)
concentration (μM)
D
topotecan
wtABCG2
Y413S
Vanadate-sensitive ATPase activity
(nmol P$_i$/ min/ mg membrane protein)
concentration (μM)

Figure 4

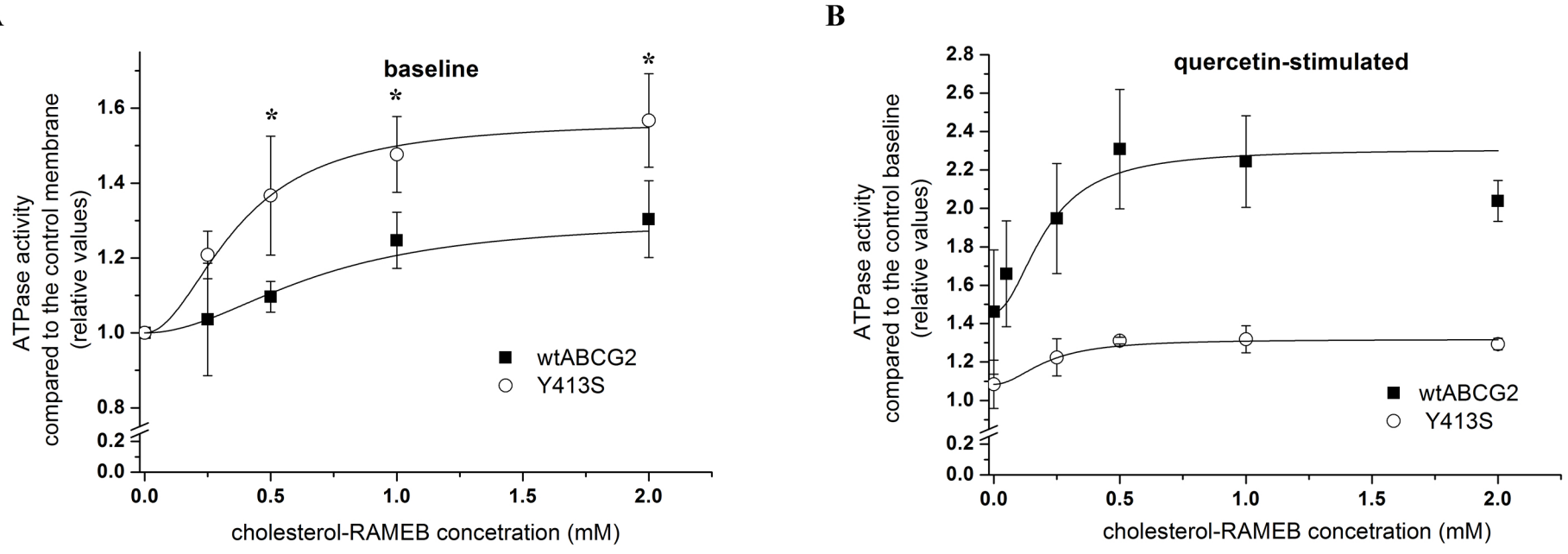
A
baseline
ATPase activity
compared to the control membrane
(relative values)
cholesterol-RAMEB concetration (mM)
wtABCG2
Y413S
*
*
*
B
quercetin-stimulated
ATPase activity
compared to the control baseline
(relative values)
cholesterol-RAMEB concetration (mM)
wtABCG2
Y413S

Figure 5

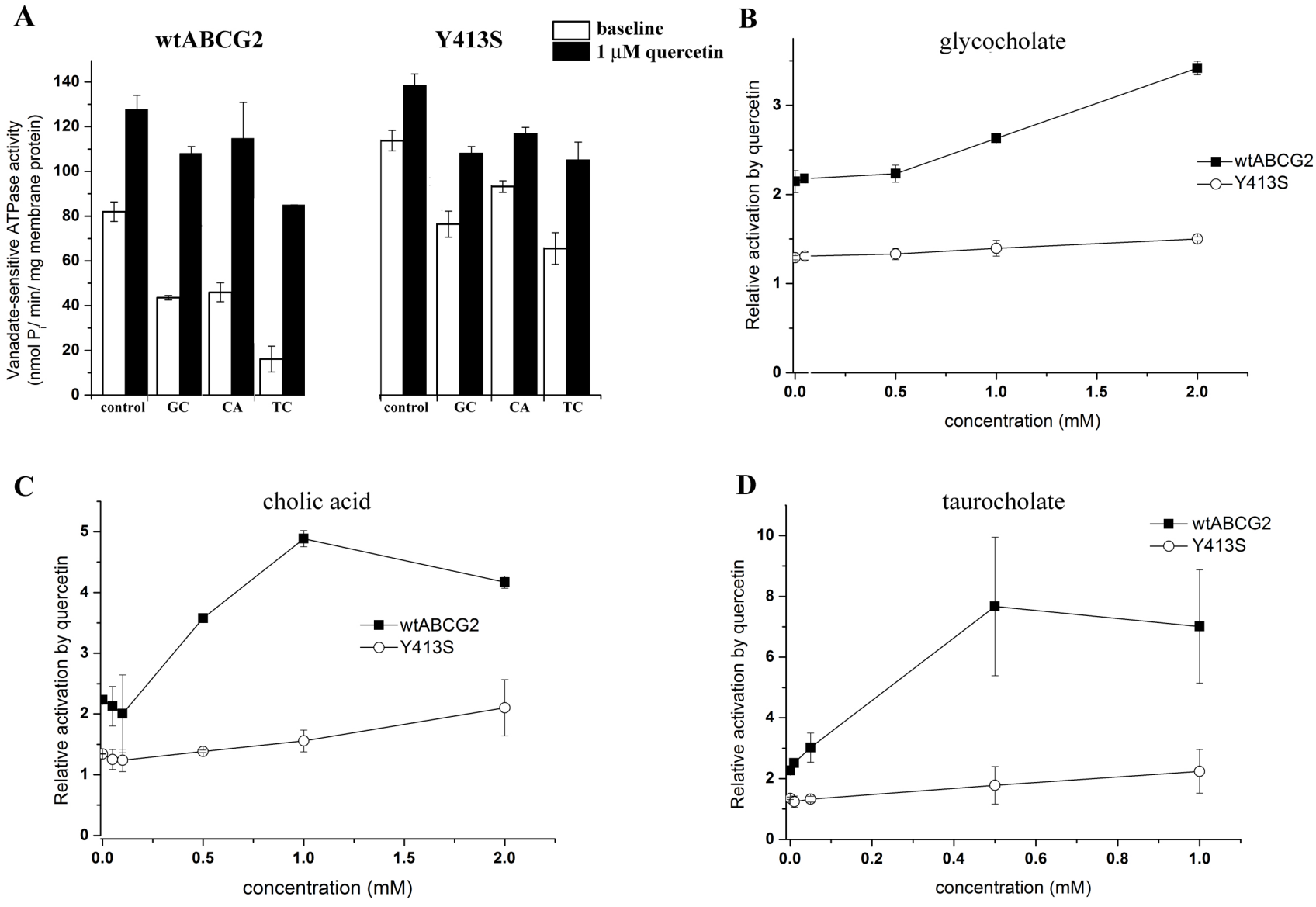
A
wtABCG2
Y413S
baseline
1 μM quercetin
Vanadate-sensitive ATPase activity
(nmol P$_i$/ min/ mg membrane protein)
control
GC
CA
TC
B
glycocholate
Relative activation by quercetin
concentration (mM)
wtABCG2
Y413S
C
cholic acid
D
taurocholate

Figure 6

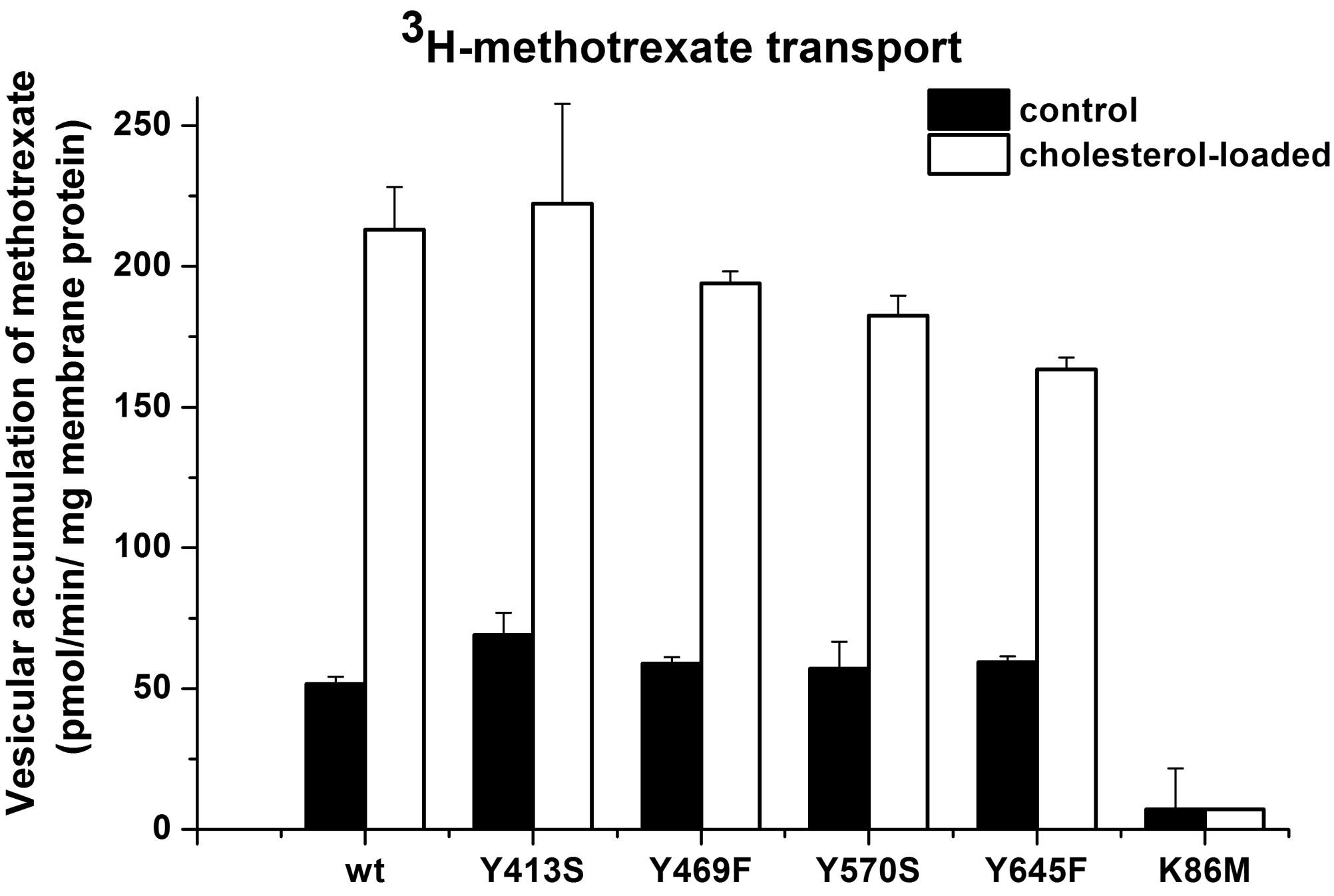
^{3}H-methotrexate transport
control
cholesterol-loaded
Vesicular accumulation of methotrexate
(pmol/min/ mg membrane protein)
250
200
150
100
50
0
wt
Y413S
Y469F
Y570S
Y645F
K86M

Figure 7

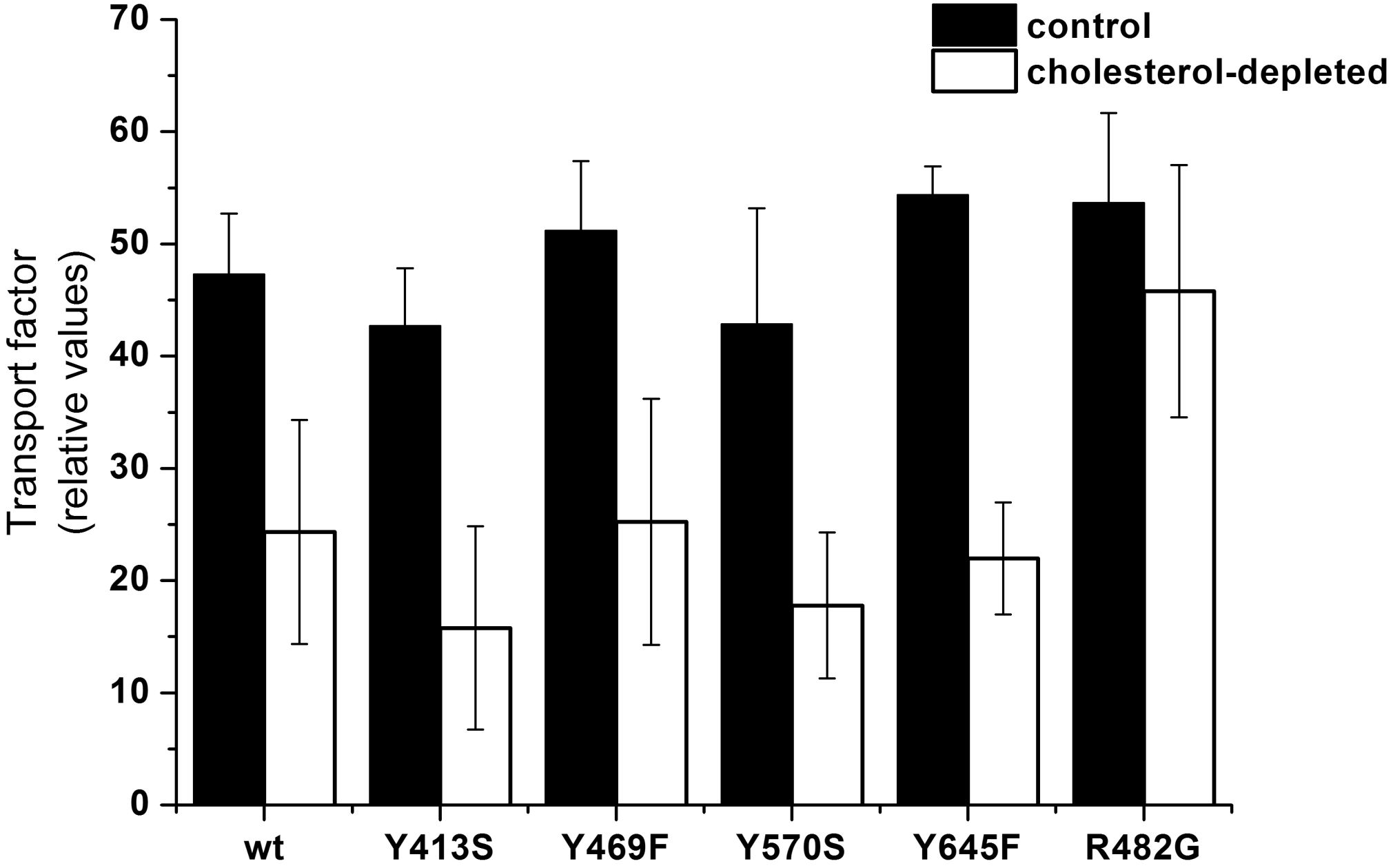
control
cholesterol-depleted
Transport factor
(relative values)
0
10
20
30
40
50
60
70
wt
Y413S
Y469F
Y570S
Y645F
R482G

Figure 8

A

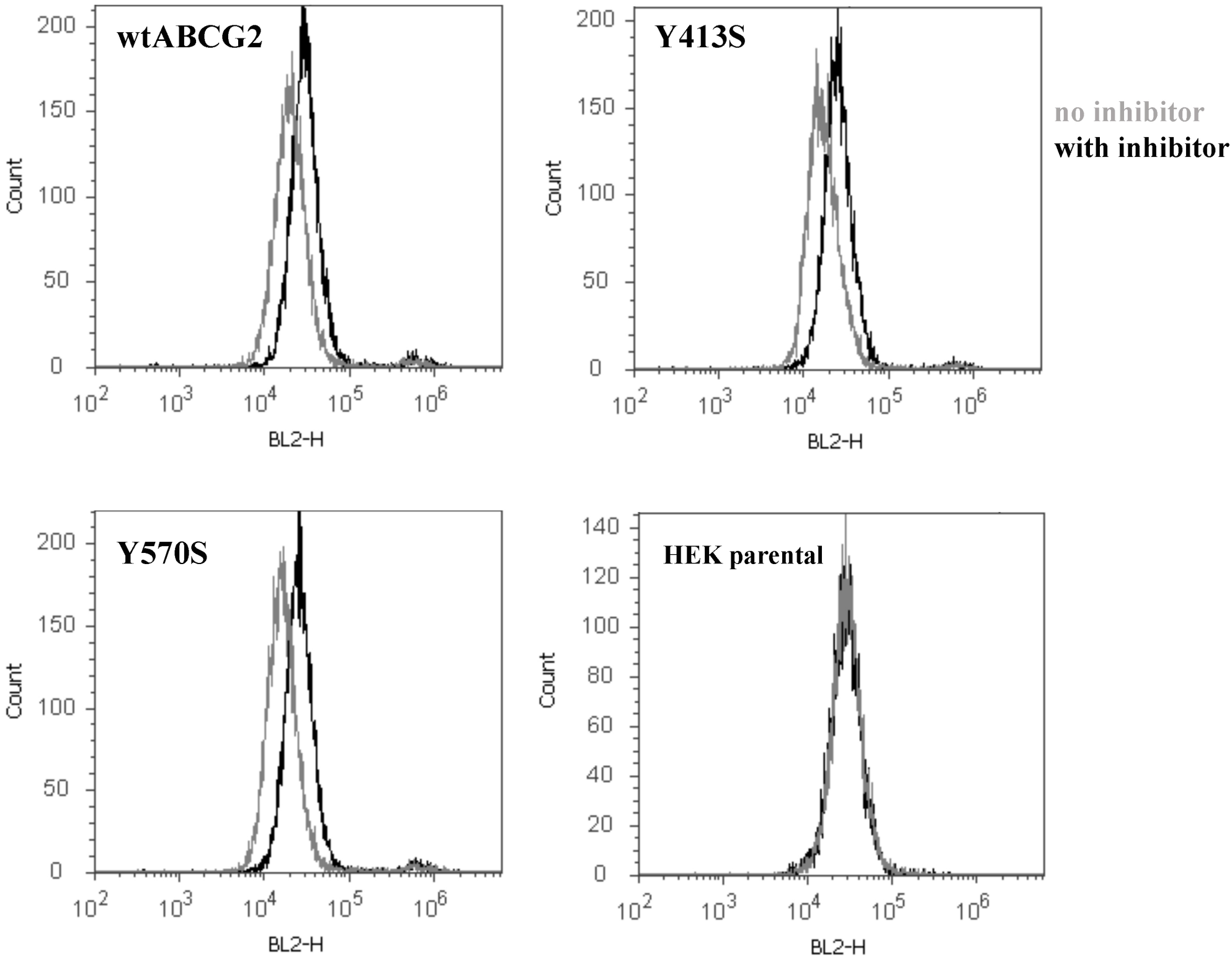
wtABCG2
Y413S
Y570S
HEK parental
Count
BL2-H
no inhibitor
with inhibitor

B

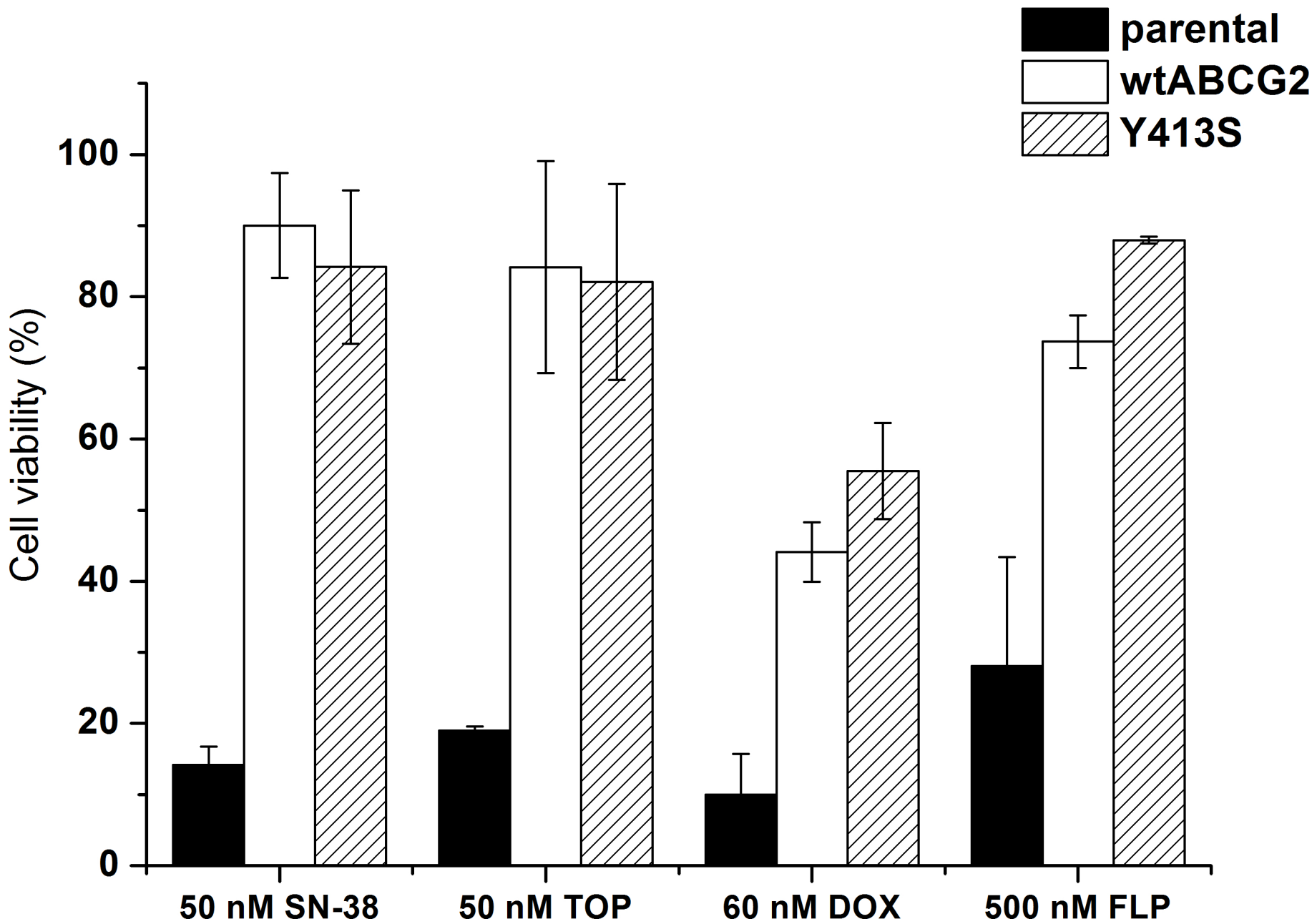
parental
wtABCG2
Y413S
Cell viability (%)
50 nM SN-38
50 nM TOP
60 nM DOX
500 nM FLP